

## ARTICLE OPEN



# $\alpha$ -Synuclein pathology in post-mortem retina and optic nerve is specific for $\alpha$ -synucleinopathies

Frederique J. Hart de Ruyter<sup>1,2</sup>, Tjado H. J. Morrema<sup>1</sup>, Jurre den Haan<sup>2</sup>, Gina Gase<sup>1</sup>, Jos W. R. Twisk<sup>3</sup>, Johannes F. de Boer<sup>4</sup>, Philip Scheltens<sup>2</sup>, Femke H. Bouwman<sup>2</sup>, Frank D. Verbraak<sup>5</sup>, Annemieke J. M. Rozemuller<sup>1</sup> and Jeroen J. M. Hoozemans<sup>1,6</sup>✉

There is increasing interest in studying retinal biomarkers for various neurodegenerative diseases. Specific protein aggregates associated with neurodegenerative diseases are present in the retina and could be visualised in a non-invasive way. This study aims to assess the specificity and sensitivity of retinal  $\alpha$ -synuclein aggregates in neuropathologically characterised  $\alpha$ -synucleinopathies, other neurodegenerative diseases and non-neurological controls. Post-mortem eyes ( $N = 99$ ) were collected prospectively through the Netherlands Brain Bank from donors with Parkinson's disease (and dementia), dementia with Lewy bodies, multiple system atrophy, Alzheimer's disease, other neurodegenerative diseases and non-neurological controls. Multiple retinal and optic nerve cross-sections were immunostained with anti- $\alpha$ -synuclein antibodies (LB509, KM51, and anti-pSer129) and assessed for aggregates and inclusions.  $\alpha$ -Synuclein was observed as Lewy neurites in the retina and oligodendroglial cytoplasmic inclusions in the optic nerve and was highly associated with Lewy body disease ( $P < 0.001$ ) and multiple system atrophy ( $P = 0.001$ ). In all multiple system atrophy cases, the optic nerve showed oligodendroglial cytoplasmic inclusions, while retinal Lewy neurites were absent, despite coincidental brain Lewy pathology. With high specificity (97%) and sensitivity (82%), retinal/optic nerve  $\alpha$ -synuclein differentiates primary  $\alpha$ -synucleinopathies from other cases and controls.  $\alpha$ -Synuclein pathology occurs specifically in the retina and optic nerve of primary  $\alpha$ -synucleinopathies as opposed to other neurodegenerative diseases—with and without  $\alpha$ -synuclein co-pathology—and controls. The absence of retinal Lewy neurites in multiple system atrophy could contribute to the development of an in vivo retinal biomarker that discriminates between Lewy body disease and multiple system atrophy.

npj Parkinson's Disease (2023)9:124; <https://doi.org/10.1038/s41531-023-00570-5>

## INTRODUCTION

The retina and optic nerve are embryonically derived from the central nervous system and show similar structural and functional characteristics to the brain<sup>1</sup>. Therefore, the retina is considered a potential source of biomarkers for neurodegenerative brain diseases. The optic nerve consists of glial cells and the axons of retinal ganglion cells, which extend as the optic tract to the lateral geniculate nucleus and superior colliculus, forming a direct connection with the brain. The retina contains ganglion cells displaying similarities with neurons of the central nervous system, interneurons, and different types of glial cells<sup>2</sup>. Existing data suggests that the retina mirrors ongoing pathology associated with neurodegenerative diseases in the brain<sup>3–10</sup>, supporting the potential of in-vivo retinal imaging as a non-invasive diagnostic approach.

Several neurodegenerative diseases are characterised by the aggregation of  $\alpha$ -synuclein ( $\alpha$ Syn) and therefore termed  $\alpha$ -synucleinopathies<sup>11</sup>.  $\alpha$ -Synucleinopathies—of which Parkinson's disease is the most common form—can be subdivided into two major classes: Lewy body disease and multiple system atrophy<sup>12,13</sup>. Lewy body disease encompasses the clinically defined entities Parkinson's disease, Parkinson's disease dementia and dementia with Lewy bodies. It is neuropathologically characterised by neuronal  $\alpha$ Syn aggregation forming Lewy bodies and Lewy neurites<sup>11</sup>. Multiple system atrophy is characterised by oligodendroglial cytoplasmic inclusions (GCIs). These neuropathological

aggregates are associated with neuronal death and demyelination<sup>14</sup>. Pathological formation of  $\alpha$ Syn aggregates are thought to be caused by the binding of cytoplasmic  $\alpha$ Syn with lipid membranes disrupting their role in regulating neurotransmission and synaptic function<sup>15,16</sup>. Lewy bodies and GCIs are primarily composed of  $\alpha$ Syn phosphorylated at serine 129 (pSer129), which is why this phosphorylated  $\alpha$ Syn epitope is considered a marker for pathology and suggested as a potential diagnostic and progression biomarker in Parkinson's disease<sup>17,18</sup>. Despite their shared presence of  $\alpha$ Syn aggregates,  $\alpha$ -synucleinopathies show significant clinical and pathological heterogeneity.

Under normal conditions,  $\alpha$ Syn is endogenously present in all retinal layers in cell bodies and processes<sup>19,20</sup>. In Parkinson's disease, native  $\alpha$ Syn was found as neuronal, globular inclusions in the inner nuclear layer and ganglion cell layer<sup>8</sup>. Since  $\alpha$ Syn pSer129 has gained interest as a key marker for pathology, different studies on the retina have reported the presence of  $\alpha$ Syn pSer129 specifically in Parkinson's disease<sup>7,9</sup> and dementia with Lewy bodies<sup>7</sup> as opposed to control cases. Ortuño-Lizarán and colleagues<sup>9</sup>, studying whole-mount retinas of Parkinson's disease cases, reported  $\alpha$ Syn pSer129 deposits resembling brain Lewy bodies.  $\alpha$ Syn pSer129 was observed in ganglion cell perikarya, axonal fibres and dendrites. Additional  $\alpha$ Syn pSer129 immunostaining on cross-sections showed inclusions in the inner nuclear and ganglion cell layers resembling characteristic Lewy bodies and neurites. Despite these significant findings, one study could

<sup>1</sup>Department of Pathology, Amsterdam UMC location Vrije Universiteit Amsterdam, De Boelelaan 1117, Amsterdam, The Netherlands. <sup>2</sup>Department of Neurology and Alzheimer Center Amsterdam, Amsterdam UMC location Vrije Universiteit Amsterdam, De Boelelaan 1117, Amsterdam, The Netherlands. <sup>3</sup>Department of Epidemiology and Data Science, Vrije Universiteit Amsterdam, De Boelelaan 1117, Amsterdam, The Netherlands. <sup>4</sup>Department of Physics and Astronomy and LaserLaB, Vrije Universiteit Amsterdam, De Boelelaan 1081, Amsterdam, The Netherlands. <sup>5</sup>Department of Ophthalmology, Amsterdam UMC location Vrije Universiteit Amsterdam, De Boelelaan 1117, Amsterdam, The Netherlands. <sup>6</sup>Amsterdam Neuroscience, Neurodegeneration, Amsterdam, The Netherlands. ✉email: [jjm.hoozemans@amsterdamumc.nl](mailto:jjm.hoozemans@amsterdamumc.nl)

**Table 1.** Group demographics of cases used in this study based on clinicopathological diagnosis.

	Controls <i>n</i> = 25	Parkinson's disease (dementia) <i>n</i> = 21	Dementia with Lewy bodies <i>n</i> = 5	Multiple system atrophy MSA-p, MSA-c/p <i>n</i> = 7	Alzheimer's disease <i>n</i> = 19	Other neurodegenerative diseases Primary tauopathies, FTLD, ALS, MS, Fragile X syndrome, vascular dementia, hydrocephalus <i>n</i> = 22
Female, <i>n</i>	18	7	3	5	12	9
Age at death mean ± SD	72 ± 16	77 ± 9	81 ± 8	70 ± 9	77 ± 9	70 ± 14
Disease duration median; min–max	n/a	192 (37–324)	72 (48–84)	60 (24–120)	108 (12–312)	84 (24–180)
Presence of visual hallucinations, <i>n</i>	0	13	5	0	1	2
Presence of dementia, <i>n</i>	0	9	3	1	16	9
Braak stage for LB median; min–max	0 (0–4)	6 (3–6)	6 (4–6)	4 (3–5)	0 (0–4)	0 (0–3)
LPC stage	0 (0–4)	5 (3–5)	5 (5)	5 (3–5)	0 (0–4)	0 (0–3)
Post-mortem interval eyes median; min–max	8 (3–30)	6 (4–10)	7 (5–10)	6 (5–9)	7 (5–16)	6 (4–18)

Data are shown as mean ± SD or median (minimum–maximum). Age at death is shown in years, disease duration in months and post-mortem interval in hours. LPC stage is shown numerically; 0, non- $\alpha$ Syn; 1, olfactory-only; 2, amygdala-predominant; 3, brainstem-predominant; 4, limbic; 5, neocortical. ALS amyotrophic lateral sclerosis, FTLD frontotemporal lobar degeneration, LB Lewy bodies, LPC Lewy pathology consensus criteria, MS multiple sclerosis, MSA-c multiple system atrophy cerebellar variant, MSA-p multiple system atrophy predominant parkinsonism.

not confirm the presence of  $\alpha$ Syn pathology in the retinas of Parkinson's disease as opposed to controls<sup>21</sup>.

It has been reported that the level of  $\alpha$ Syn pathology in the retina correlated positively with the severity of Parkinson's disease and may therefore serve as a biomarker for the disease<sup>9</sup>. In-vivo examination of  $\alpha$ Syn in the retina may provide insight into the pathogenesis of  $\alpha$ -synucleinopathies and the potential efficacy of therapeutic interventions. While previous studies have already established the presence of Lewy pathology in the retina in Parkinson's disease<sup>7,9</sup>, dementia with Lewy bodies<sup>7</sup> and incidental Lewy body disease<sup>9</sup>, the ophthalmologic occurrence of  $\alpha$ Syn in multiple system atrophy has not been reported before. Moreover, it remains unclear whether  $\alpha$ Syn is present in the retina of cases with other neurodegenerative diseases and with  $\alpha$ Syn co-pathology in the brain, for instance, in the presence of incidental, amygdala-only  $\alpha$ Syn pathology<sup>22</sup>. This study evaluated the presence of ophthalmologic  $\alpha$ Syn pathology in a large cohort with different neurodegenerative diseases, including primary  $\alpha$ -synucleinopathies and other neurodegenerative disorders with and without  $\alpha$ Syn co-pathology, and non-neurological controls.

## RESULTS

### Cohort description

Individual case details are reported in Supplementary Tables 1 and 2, and group demographics based on neuropathological diagnosis are described in Table 1. No significant group difference was found for age at death ( $P = 0.16$ ), sex ( $P = 0.08$ ) or post-mortem interval ( $P = 0.06$ ). Parkinson's disease (dementia) had a significantly higher disease duration than all other groups ( $P < 0.001$ ). A significant difference was found between groups for visual hallucinations and dementia ( $P < 0.001$ ).  $\alpha$ -Synucleinopathies had a significantly higher Braak LB stage ( $P < 0.001$ ) and LPC stage ( $P < 0.001$ ).

### Morphological appearance of $\alpha$ -synucleinopathy in the retina and optic nerve

Mesencephalon tissue of a Parkinson's disease case was immunostained with LB509 (Fig. 1a), pSer129 (Fig. 1b) and KM51 (Fig. 1c) as a positive control. In three  $\alpha$ -synucleinopathy cases (#35, #36, #42), immunostaining with pSer129 and LB509 showed a sporadic cytoplasmic inclusion in cells within the ganglion cell layer (Fig. 1d), which was also visualised using anti-NeuN (Fig. 1d'). Lewy-like neurites were seen in the retinal nerve fibre layer and inner plexiform layer of the retina (Fig. 1e) as assessed with LB509, pSer129 and KM51. No visual differences were observed in the appearance of Lewy-like neurites using these three antibodies. Immunohistochemistry with all three antibodies also revealed pathological structures in the optic nerve (Fig. 1f). Here,  $\alpha$ Syn pathology was mainly observed as cellular inclusions, specifically in cases with multiple system atrophy resembling GCIs (Fig. 1g), which was also shown by double-labelling with a marker for oligodendrocytes using anti-SOX10 (Fig. 1h). Optic nerve tissue showed  $\alpha$ Syn pathology resembling GCIs in all six multiple system atrophy cases, as opposed to other cases with optic nerve tissue ( $n = 22$ ). Moreover, although all multiple system atrophy cases had additional Lewy body brain pathology, only two of them (#54, #55) also showed neurites in the optic nerve head at the level of the lamina cribrosa (Fig. 1f, i). In contrast, none showed pathology resembling Lewy neurites in the retina.

### Specific occurrence of $\alpha$ Syn pathology in the retina and optic nerve in synucleinopathies

$\alpha$ Syn pathology was assessed in the retina and optic nerve in different clinicopathological groups (Fig. 2). For this analysis,  $\alpha$ Syn pathology in the retina and optic nerve was combined, resulting in a total score to gain an inclusive interpretation of the pathologic manifestation per case (Supplementary Table 2).  $\alpha$ Syn pathology in the retina/optic nerve was primarily seen in cases with a primary  $\alpha$ -synucleinopathy (Fig. 2). The highest ratio was seen for

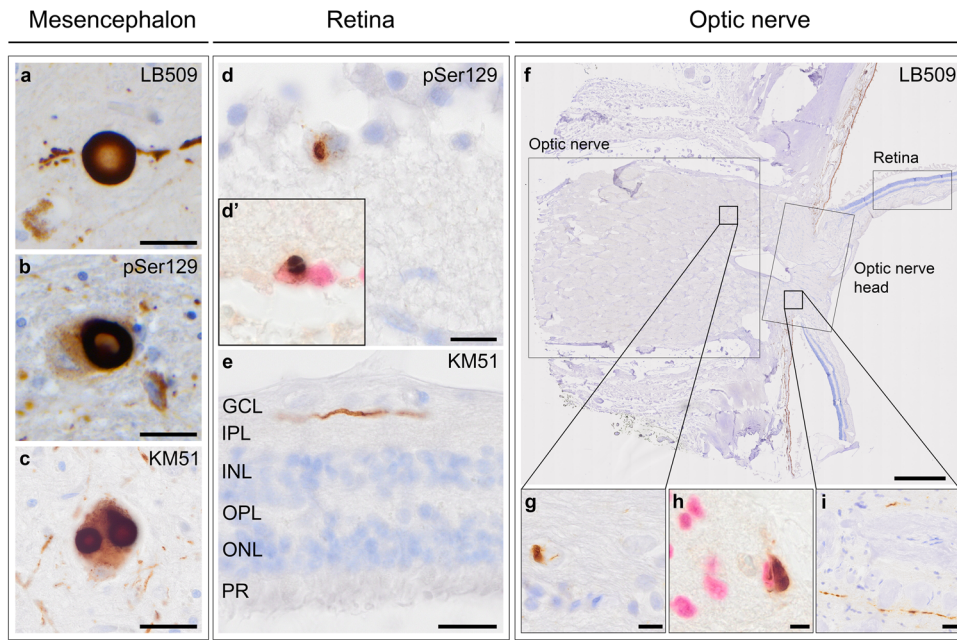


**Fig. 1 Localisation and morphology of  $\alpha$ Syn pathology in the retina and optic nerve.** Mesencephalon of a Parkinson's disease case was used as a positive control, here showing immunostaining with **a** LB509, **b** pSer129 and **c** KM51. **d** pSer129 showed a neuronal staining in a ganglion cell located in the GCL of the retina of a Parkinson's disease dementia case. **d'**  $\alpha$ Syn cytoplasmic inclusion (brown) in a ganglion cell was also observed with a nuclear staining for ganglion cells using NeuN (Liquid Permanent Red). **e** Lewy-like neurites were observed in the IPL of a Parkinson's disease dementia case. **f-h** The optic nerve showed  $\alpha$ Syn cytoplasmic inclusions in multiple system atrophy (#54). **h**  $\alpha$ Syn cytoplasmic inclusions were observed in oligodendrocytes by co-labelling with anti-SOX-10, which labels nuclei of oligodendrocytes (Liquid Permanent Red). **i** Multiple system atrophy cases additionally showed Lewy-like neurites in the optic nerve head (#54). Immunostaining is shown with DAB (brown), and nuclei are counterstained with haematoxylin (blue). In (**d'**) and (**h**), nuclei are immunolabelled and stained with Liquid Permanent Red. Scale bars: **a-c**, **e**, **i** = 20  $\mu$ m, **d**, **g** = 10  $\mu$ m, **f** = 800  $\mu$ m, **h** = 5  $\mu$ m. GCL ganglion cell layer, IPL inner plexiform layer, INL inner nuclear layer, OPL outer plexiform layer, ONL outer nuclear layer, PR photoreceptors.

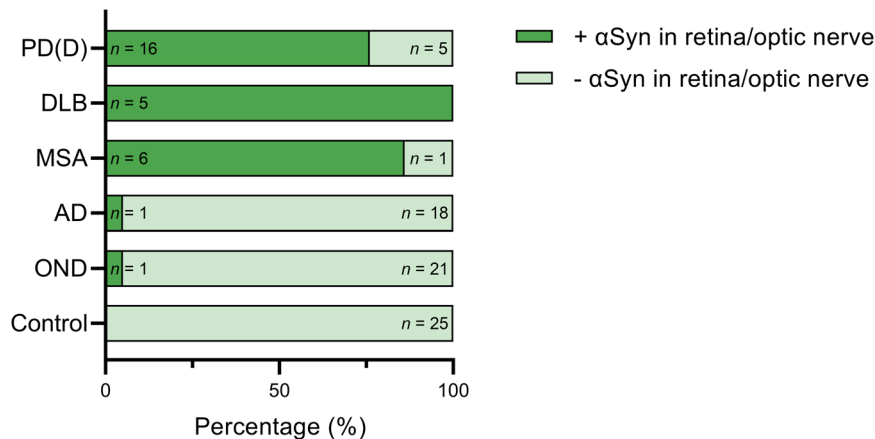


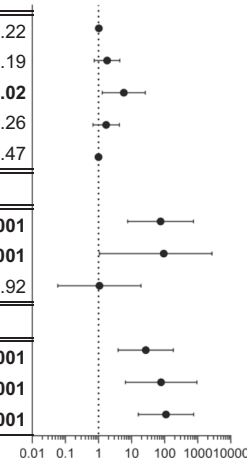
**Fig. 2 Presence of retinal/optic nerve  $\alpha$ Syn pathology in different clinicopathological subgroups.** Shown is the percentage of cases with  $\alpha$ Syn pathology (dark green indicates presence, light green indicates absence) in the retina/optic nerve per subgroup. The highest percentage of cases with  $\alpha$ Syn pathology in the retina/optic nerve is seen in dementia with Lewy bodies (DLB) (100%), followed by multiple system atrophy (MSA) (86%) and Parkinson's disease (dementia) (PD(D)) (76%). Additionally, one Alzheimer's disease (AD) and one FTLD-tau (OND) case, both with substantial  $\alpha$ Syn pathology in the brain, showed  $\alpha$ Syn pathology in the retina/optic nerve. Of the Parkinson's disease (dementia) cases, 18% had no  $\alpha$ Syn pathology in the retina or optic nerve. One multiple system atrophy case had no optic nerve tissue available (#58). This case showed no  $\alpha$ Syn pathology in the retina, similar to the other multiple system atrophy cases. PD(D) Parkinson's disease (dementia), DLB dementia with Lewy bodies, MSA multiple system atrophy, AD Alzheimer's disease, OND other neurodegenerative diseases, *n* number.

dementia with Lewy bodies (5/5), followed by multiple system atrophy (6/7) and Parkinson's disease (dementia) (16/21). Also, one Alzheimer's disease (1/19; #65) and one frontotemporal lobar degeneration-tau case (1/22; #83) showed  $\alpha$ Syn pathology in the form of Lewy neurites in the retina/optic nerve, both of which had substantial  $\alpha$ Syn co-pathology in the brain (Braak LB stage IV and III, respectively). None of the non-neurological controls (0/25)

showed  $\alpha$ Syn pathology in the retina/optic nerve. Although a large proportion of Parkinson's disease (dementia) cases showed corresponding  $\alpha$ Syn pathology in the retina/optic nerve, four out of 11 Parkinson's disease cases (#27, #28, #31, #45) and one out of 10 Parkinson's disease dementia cases (#29) did not. On a group level, a significant association was found between  $\alpha$ Syn pathology in the retina/optic nerve and primary  $\alpha$ -synucleinopathies (i.e.

**Table 2.** Univariable logistic regression analyses predicting the likelihood of  $\alpha$ Syn pathology in the retina/optic nerve.

Variable	Odds ratio	95% CI odds ratio	P value
Age at death	1.02	0.99 - 1.06	0.22
Sex	1.81	0.75 - 4.38	0.19
Visual hallucinations	5.82	1.30 - 25.97	<b>0.02</b>
Dementia	1.70	0.68 - 4.20	0.26
Disease duration	1.00	1.00 - 1.01	0.47
<i>Diagnostic group<sup>1</sup></i>			
Lewy body disease	80.98	8.13 - 806.15	<b>&lt;.001</b>
Multiple system atrophy	142.85	7.01 - 2911.53	<b>0.001</b>
Alzheimer's disease	1.15	0.06 - 20.88	0.92
<i>Braak LB stage<sup>2</sup></i>			
Braak stage IV	28.72	4.24 - 194.61	<b>&lt;.001</b>
Braak stage V	84.59	7.04 - 1016.25	<b>&lt;.001</b>
Braak stage VI	116.18	16.91 - 798.29	<b>&lt;.001</b>



Statistical analysis was performed using univariable binary logistic regression. The Forest plot graphs the odds ratio with the 95% confidence intervals of the different variables. The axis scale is logarithmic with log-spaced ticks.

LB Lewy body.

<sup>1</sup>Other neurodegenerative diseases group is used as reference.

<sup>2</sup>Braak LB 0-III is used as reference.

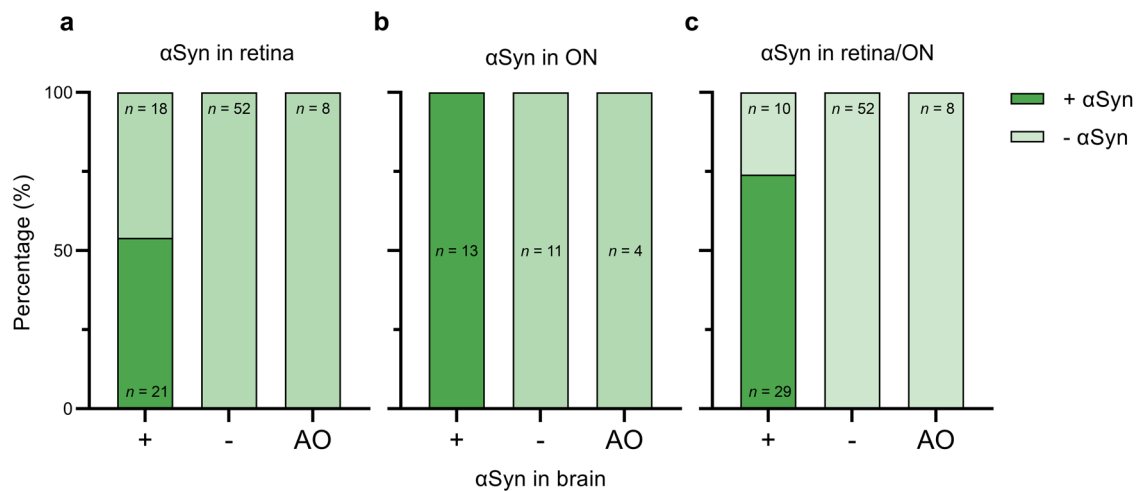


**Fig. 3 Presence of  $\alpha$ Syn pathology in the retina and optic nerve in cases with  $\alpha$ Syn pathology in the brain, cases without  $\alpha$ Syn pathology in the brain and amygdala-only  $\alpha$ Syn pathology.** Shown is the percentage of cases with  $\alpha$ Syn pathology (dark green indicates presence, light green indicates absence) in **a** retina, **b** optic nerve and **c** retina/optic nerve combined in cases with (+), without (-) and amygdala-only (AO)  $\alpha$ Syn pathology in the brain. **a** 54% of the cases with  $\alpha$ Syn pathology in the brain (+) showed  $\alpha$ Syn pathology in the retina versus 0% of the cases without  $\alpha$ Syn pathology in the brain (-) or with amygdala-only (AO)  $\alpha$ Syn pathology. **b** Of cases with optic nerve tissue available ( $n = 28$ ), all clinicopathological  $\alpha$ -synucleinopathies (+;  $n = 13$ ) showed  $\alpha$ Syn pathology in the optic nerve as opposed to none of the other cases ( $n = 15$ ). **c** Of the cases with  $\alpha$ Syn in the brain ranging from brainstem-predominant to neocortical, 74% showed  $\alpha$ Syn pathology in the retina/optic nerve. All cases without  $\alpha$ Syn in the brain (-;  $n = 52$ ) showed the absence of  $\alpha$ Syn pathology in the retina/optic nerve, as did the cases with amygdala-only  $\alpha$ Syn pathology (AO;  $n = 8$ ). ON optic nerve, AO amygdala-only,  $n$  number.

Lewy body disease and multiple system atrophy), where the highest odds ratio was found for multiple system atrophy ( $P = 0.001$ ; Table 2). Calculating the accuracy of  $\alpha$ Syn pathology in the retina/optic nerve for identifying the presence of a primary  $\alpha$ -synucleinopathy yielded a sensitivity of 82% and specificity of 97%, with a positive predictive value of 93% and a negative predictive value of 91%.

Further exploring the relation between  $\alpha$ Syn pathology in the retina and optic nerve versus the presence of  $\alpha$ Syn pathology in

the brain, the optic nerve was found to be more accurately associated with the presence of  $\alpha$ Syn in the brain than the retina (negative predictive value of 100% for the optic nerve versus 74% for the retina), as is shown in Fig. 3. As depicted here, 54% of the cases with  $\alpha$ Syn pathology in the brain showed  $\alpha$ Syn pathology in the retina (Fig. 3a) versus 100% in the optic nerve (Fig. 3b). When dichotomous scores of the retina and optic nerve were combined, 74% of the cases with  $\alpha$ Syn pathology in the brain also showed  $\alpha$ Syn pathology in the retina/optic nerve (Fig. 3c). None of the

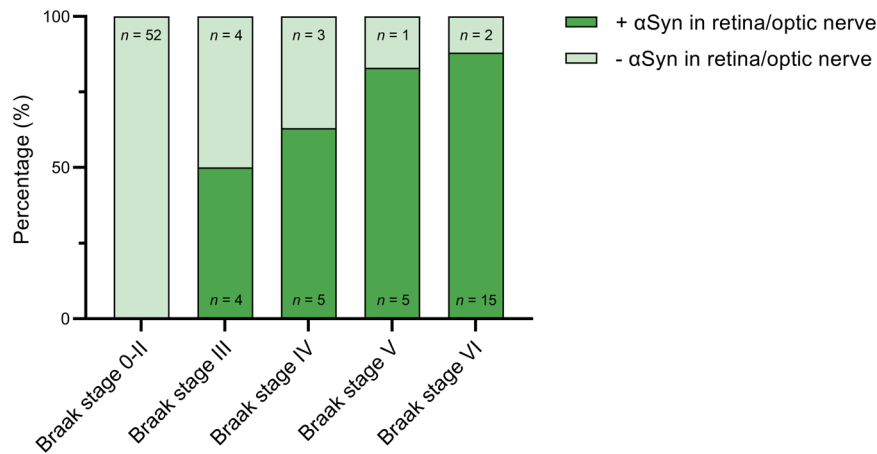


**Fig. 4 Relation between  $\alpha$ Syn pathology in the retina/optic nerve and Braak LB stage.** Shown is the percentage of cases with  $\alpha$ Syn pathology (dark green indicates presence, light green indicates absence) in the retina/optic nerve in different Braak stages.  $\alpha$ Syn pathology in the retina/optic nerve was not observed in cases with lower Braak stages ranging from 0 to II. With increasing Braak stage,  $\alpha$ Syn pathology in the retina/optic nerve gradually increased and was most frequently seen in cases with Braak stage V/VI.

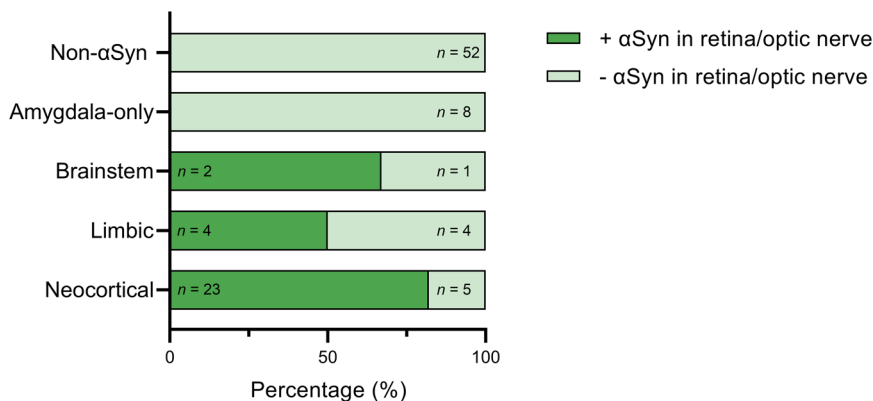


**Fig. 5 Relation between  $\alpha$ Syn pathology in the retina/optic nerve and the LPC staging system.** Shown is the percentage of cases with  $\alpha$ Syn pathology (dark green indicates presence, light green indicates absence) in the retina/optic nerve in different stages of  $\alpha$ -synucleinopathy according to the LPC staging system.  $\alpha$ Syn pathology in the retina/optic nerve was absent in cases without  $\alpha$ Syn in the brain (non- $\alpha$ Syn) and with amygdala-only  $\alpha$ Syn presence. Cases that did have  $\alpha$ Syn pathology in the retina/optic nerve had an LPC stage of brainstem-predominant (67%), limbic (50%) or neocortical (82%). LPC Lewy pathology consensus criteria.

amygdala-only cases showed  $\alpha$ Syn pathology in the retina or optic nerve. In addition, none of the cases without  $\alpha$ Syn in the brain ( $n = 52$ ) showed  $\alpha$ Syn pathology in the retina or optic nerve, indicating a high specificity.

#### **$\alpha$ Syn pathology in the retina/optic nerve correlates with $\alpha$ Syn pathology in the brain**

Whether there was a significant association between  $\alpha$ Syn pathology in the retina/optic nerve and the spread of  $\alpha$ Syn pathology in the brain was analysed using the Braak (Fig. 4) and LPC staging systems (Fig. 5). Logistic regression analysis indicated that the likelihood of finding  $\alpha$ Syn pathology in the retina/optic nerve increased with Braak stage with the highest odds ratio for stage VI ( $P < 0.001$ ) (Table 2). Notably, eight cases had amygdala-only  $\alpha$ Syn presence and could not be classified within the Braak staging system. The occurrence of  $\alpha$ Syn pathology within the different stages of LPC is shown in Fig. 5, illustrating the absence of  $\alpha$ Syn pathology in the retina/optic nerve in cases without  $\alpha$ Syn presence in the brain and in cases with amygdala-only  $\alpha$ Syn presence. Because no data was available on cases with olfactory-only  $\alpha$ Syn presence, and none of the amygdala-only cases showed  $\alpha$ Syn pathology in the retina or optic nerve, logistic regression

analysis could not assess the association with the LPC staging system.

In addition, the relation between clinical variables and the presence of  $\alpha$ Syn pathology in the retina/optic nerve was studied (Table 2). Corrected for age at death, sex and  $\alpha$ Syn in the brain, visual hallucinations were significantly related to  $\alpha$ Syn pathology in the retina/optic nerve ( $P = 0.02$ ), whereas dementia and disease duration were not.

#### **DISCUSSION**

Developing retinal biomarkers for various neurodegenerative diseases requires understanding of the retina and optic nerve pathology and the connection with neuropathology in the brain. In this post-mortem study, the prevalence of  $\alpha$ Syn pathology in the retina and optic nerve was assessed in a well-characterised cohort with different neurodegenerative diseases and non-neurological controls.  $\alpha$ Syn pathology was mainly observed in the retina and optic nerve of primary  $\alpha$ -synucleinopathies as opposed to other neurodegenerative disorders and controls without  $\alpha$ Syn in the brain. There is a high specificity (97%) and sensitivity (82%) for the presence of  $\alpha$ Syn in the retina and optic nerve in relation to brain  $\alpha$ Syn pathology as part of a primary  $\alpha$ -



synucleinopathy. Results from this study suggest that  $\alpha$ Syn pathology in the retina and optic nerve is associated with the distribution of  $\alpha$ Syn pathology according to the Braak LB stage and thus mirrors the pathological presence of  $\alpha$ Syn in the brain.

The observation of  $\alpha$ Syn pathology in the retina and optic nerve tissue of cases with  $\alpha$ -synucleinopathies is in concordance with previous studies<sup>7–9</sup>. In the present study,  $\alpha$ Syn pathology was observed as Lewy neurites in the retina and optic nerve and as GCIs in the optic nerve. Sporadically and only in primary synucleinopathy cases, cytoplasmic inclusions were observed in the ganglion cell layer, presumably in ganglion cells. These structures resemble what was earlier described as Lewy body-like inclusions<sup>9</sup>. However, retinal cytoplasmic inclusions observed in the present study did not show similarity with the classic halo-morphology seen in the brain, nor were they similar in size. The absence of classic Lewy bodies in this study suggests that the retina differs from the brain in response mechanisms to  $\alpha$ Syn-associated pathology and may hold essential qualities such as a highly metabolic environment aimed at preventing the formation of protein aggregation until the stage of classic inclusion bodies<sup>23</sup>.

Although previous studies<sup>7–10,21,24</sup>, reported on the presence and characterisation of  $\alpha$ Syn pathology in the retina in  $\alpha$ -synucleinopathies,  $\alpha$ Syn pathology in multiple system atrophy had not yet been described. Multiple system atrophy cases showed  $\alpha$ Syn pathology in the form of cytoplasmic inclusion bodies resembling GCIs in the optic nerve, which were not observed in other cases with optic nerve tissue available. In-vivo optical coherence tomography data support optic nerve pathology in multiple system atrophy. In their review, Mendoza-Santesteban and colleagues<sup>25</sup> outlined data on patients with multiple system atrophy that show a specific pattern of damage of the post-laminar myelinated optic nerve axons. They describe damaging of the M-cell axons arising from the peripheral retina and the sparing of the P-cell axons originating from the macular area. This leads to retinal nerve fibre layer thinning around the optic nerve head in the superior, nasal and inferior quadrant, but not in the temporal quadrant, as opposed to the more general retinal nerve fibre layer thinning seen in Parkinson's disease cases. The high specificity and sensitivity found in the present study for GCI pathology in the optic nerve with relation to the presence of multiple system atrophy-associated brain pathology, and the absence of Lewy pathology in the retinas of these cases, makes the eye an exciting candidate in the search for biomarkers that can discriminate between  $\alpha$ -synucleinopathies.

We found a clear relation between Lewy pathology in the retina/optic nerve and  $\alpha$ Syn pathology in the brain. Nonetheless, in 18% of the primary  $\alpha$ -synucleinopathy cases, no  $\alpha$ Syn pathology in the retina or optic nerve was observed. One explanation for the absence of  $\alpha$ Syn pathology could be that pathology was missed due to a Type II error in assessing cross-sections. On the other hand, the lack of  $\alpha$ Syn pathology may suggest that the neuronal tissue of the eye is differently involved within the hierarchical spreading of  $\alpha$ Syn pathology in the brain. In a recent review by Jellinger<sup>26</sup>, evidence was outlined for multiple routes of disease progression that are different from Braak's proposed caudorostral pathway<sup>27</sup>, and that pathological progression may vary between subtypes. The pathological variability of ophthalmologic  $\alpha$ Syn seen in this study could be explained by this heterogeneity among  $\alpha$ -synucleinopathies. The significant association with the Braak LB staging system suggests that  $\alpha$ Syn pathology in the retina/optic nerve does depend on localisation and/or load of  $\alpha$ Syn pathology in the brain. In particular, the strong association with stage VI and the high proportion of cases with  $\alpha$ Syn pathology in the retina/optic nerve within the neocortical LPC stage suggests that  $\alpha$ Syn pathology in the retina/optic nerve may predict neocortical  $\alpha$ Syn involvement.

Ophthalmologic  $\alpha$ Syn was also present in one Alzheimer's disease and one frontotemporal lobar degeneration-tau case,

showing substantial  $\alpha$ Syn pathology in the brain. More interestingly, all Alzheimer's disease cases with amygdala-predominant  $\alpha$ Syn presence did not show  $\alpha$ Syn pathology in the retina or optic nerve. A recent post-mortem study demonstrates distinct distribution patterns of Lewy body pathology in the presence of Alzheimer's disease<sup>28</sup>. The authors state that amygdala-predominant Lewy bodies are Alzheimer's disease interacting pathologies as opposed to brainstem and limbic Lewy bodies. This would explain the absence of  $\alpha$ Syn pathology in the retina and optic nerve of cases with amygdala-only  $\alpha$ Syn pathology and suggests that the eye has a disease-specific involvement in the spread of  $\alpha$ Syn pathology of the brain.

Interestingly, a significant association was observed between  $\alpha$ Syn pathology in the retina/optic nerve and visual hallucinations. Given the phenomenologically complex nature of the hallucinations of subjects in this cohort, it is likely that the underlying cause lies in the presence of cortico-cerebral  $\alpha$ Syn pathology rather than ophthalmologic  $\alpha$ Syn pathology<sup>29</sup>. To understand the association between complex visual hallucinations as seen in Lewy body disease and  $\alpha$ Syn pathology in the retina and optic nerve, future studies should focus on the possibility of hierarchical spreading of  $\alpha$ Syn pathology along the retino-geniculo-cortical pathway<sup>30,31</sup>.

A strength of this study is that multiple antibodies detecting different epitopes were used to assess ophthalmologic  $\alpha$ Syn pathology. Additionally, besides the retina, also optic nerve tissue was assessed. Data from this study indicate that  $\alpha$ Syn pathology is more prominent in the optic nerve and optic nerve head than in the retina. Therefore, future studies should focus on exploring the optic nerve head, including the lamina cribrosa in addition to the retina, to develop methods for detecting  $\alpha$ Syn pathology using in-vivo scanning modalities. A limitation of this study is that only cross-sections and not whole-mount retinas were assessed, and pathology could have been missed, potentially causing a Type II error.

In conclusion, this study on a mixed cohort of neurodegenerative diseases and non-neurological controls demonstrates that the detection of  $\alpha$ Syn pathology in the retina and optic nerve shows a high specificity (97%) and sensitivity (82%) regarding the presence of primary  $\alpha$ -synucleinopathy of the brain.  $\alpha$ Syn pathology in the retina and optic nerve correlates with Lewy body disease and multiple system atrophy as opposed to Alzheimer's disease and other neurodegenerative diseases and is associated with higher Braak LB stages. Here, we report that the hallmark GCI pathology observed in the brain in cases of multiple system atrophy is also detected in the optic nerve. The absence of Lewy pathology in the retina in multiple system atrophy could contribute to developing an in-vivo biomarker discriminating between multiple system atrophy and other  $\alpha$ -synucleinopathies. The results of this study support the development of retinal biomarkers for neurodegenerative diseases such as  $\alpha$ -synucleinopathies.

## METHODS

### Post-mortem tissue

Post-mortem eyes and brain tissue of 99 donors were collected from 2009 until 2022 by the Netherlands Brain Bank<sup>32</sup> (Amsterdam, The Netherlands, <https://www.brainbank.nl>). The VUmc medical ethics committee approved the Netherlands Brain Bank donor programme (reference# 2009/148). All donors consented in writing to use their tissue and clinical records for research purposes in compliance with ethical standards. Brain autopsies were performed according to the Code of Conduct of Brain Net Europe<sup>33</sup>.

Brain autopsy was performed within 12 h post-mortem, after which brain tissue was formalin-fixed (10%; 4 weeks) and embedded in paraffin. Neuropathological diagnosis was performed (AR) according to the guidelines of the BrainNet Europe

Consortium<sup>34</sup>, including assessment of Braak-stage for Lewy bodies (Braak LB stage)<sup>27</sup> and Alzheimer's disease neuropathological changes<sup>35</sup>, including Thal-phase for A $\beta$ <sup>36,37</sup>, Braak-stage for NFTs<sup>38</sup> and CERAD score for neuritic plaque pathology<sup>39</sup>. Cases were grouped according to clinicopathological diagnosis in Parkinson's disease (and dementia)<sup>40,41</sup> ( $n = 21$ ), dementia with Lewy bodies ( $n = 5$ )<sup>42</sup>, Multiple system atrophy ( $n = 7$ ), Alzheimer's disease<sup>37</sup> ( $n = 19$ ), other neurodegenerative diseases<sup>43–45</sup> ( $n = 22$ ) and non-neurological controls ( $n = 25$ ). During screening, 12 cases were found to have a medical history of ophthalmologic disease, including glaucoma ( $n = 5$ ), age-related macular degeneration ( $n = 3$ ), optic neuritis ( $n = 1$ ), retinal detachment ( $n = 2$ ) and macular pucker ( $n = 1$ ). This was, however, not an exclusion criterion for this study. Cohort characteristics are shown in Supplementary Table 1.

### Post-mortem retinal tissue preparation

Post-mortem enucleated eyes were directly collected in 4% paraformaldehyde (PFA) and stored for 48 h before further processing (Supplemental Table 1). Some eyes were initially cryopreserved and stored for later use. In short, these eyes were frozen using isopentane at  $-90^{\circ}\text{C}$  and stored at  $-80^{\circ}\text{C}$ . To prevent damage to the retina caused by the pressure of frozen tissue, the cornea and lens were removed before freezing, which allowed for the expansion of vitreous humour. Consequently, tissue-tek O.C.T. compound (Sakura, Tokyo, Japan) was used to fill the eyeball to compensate for vitreous humour loss, to avoid folding of the eyeball during the freezing process, and to prevent direct contact between the retinal tissue and isopentane. Isopentane, an effective cryoprotectant, prevented cryo-artefacts from ice crystal formation during freezing. Frozen eyes were defrosted at room temperature (RT) in PFA for 48 h before dissection. PFA fixed eyes were dissected through the horizontal and vertical axis, resulting in temporal–superior, temporal–inferior, nasal–superior and nasal–inferior quadrants as previously described<sup>4,5</sup>.

### Immunohistochemistry

Tissue sections (10  $\mu\text{m}$  thickness) from formalin-fixed, paraffin-embedded retina of the superior and inferior axis were sequentially mounted on TOMO glass slides (Matsunami, Osaka, Japan). Brain tissue sections (7  $\mu\text{m}$  thickness) were mounted on Superfrost plus glass slides (VWR, Pennsylvania, USA). In all cases, according to the protocol of the BrainNet Europe Consortium<sup>34</sup>, the cortico-cerebral presence of  $\alpha\text{Syn}$  pathology immunostained with KM51 against full-length  $\alpha\text{Syn}$  (Novocastra/NCL-ASYN, clone KM51, RRID: AB\_442103) was assessed in the brainstem (mesencephalon, medulla oblongata, pontine tegmentum, substantia nigra) and limbic system (amygdala, middle hippocampus at the geniculate body). Clinicopathological suspected  $\alpha\text{-synucleinopathies}$  were additionally assessed in the neocortex (temporal pole, medial frontal gyrus, inferior parietal lobe, occipital pole V1/V2). Sections were air-dried overnight at  $37^{\circ}\text{C}$  before staining. Sections were deparaffinised and rehydrated using sequential incubations in xylene, alcohol and water. Endogenous peroxidase activity was suppressed by incubating the sections with 0.3%  $\text{H}_2\text{O}_2$  in phosphate buffer saline (PBS; pH 7.4) for 30 min. Antigen retrieval was performed in 10 mM/L citrate buffer (pH 6.0) and heated using an autoclave (20 min at  $121^{\circ}\text{C}$ ). Retina sections immunostained with KM51 (dilution 1:100) and LB509 (epitope from Lewy bodies purified from DLB patients, Invitrogen, 1:500, RRID: AB\_2920932) were additionally pre-treated with 100% formic acid (10 min at RT) and washed with PBS. Sections were incubated overnight at RT with primary antibodies LB509, KM51 and anti- $\alpha\text{Syn}$  pSer129<sup>46</sup> (ABCAM, Cambridge, UK, 1:100, RRID: AB\_869973) diluted in antibody diluent (Sigma-Aldrich, Saint Louis, USA). Omission of the primary antibody was used as a negative control,

and mesencephalon tissue from a Parkinson's disease case was used as a positive control. After primary antibody incubation, the sections were washed with PBS, incubated with anti-mouse/rabbit HRP Envision (DAKO, Glostrup, Denmark) (30 min) and subsequently washed using PBS. 3,3'-Diaminobenzine (DAB; DAKO) was used as a chromogen for colour development (5 min at RT). Sections were counterstained with haematoxylin, dehydrated using alcohol and xylene and mounted using Quick-D (Klinipath; Duiven, The Netherlands).

### Immunohistochemical double labelling

Tissue sections were stained for the  $\alpha\text{Syn}$  markers (LB509, KM51 and pSer129) as described above. After DAB treatment, antibody complexes were removed by heating the sections in citrate buffer using a microwave (10 min, close to boiling point). The tissue sections were incubated with either anti-SOX10 (Cell Marque 1:100, clone EP268, RRID: 2941085) or anti-NeuN (Abcam, 1:500, RRID: AB\_2532109) for 1 h at room temperature. An alkaline phosphatase (AP)-conjugated goat anti-rabbit Ig (SouthernBiotech 1:250, RRID: AB\_2722612) was incubated for 1 h, and colour development was performed using Liquid Permanent Red (DAKO). Tissue sections were mounted using Aquatex aqueous mounting medium (Merck, Darmstadt, Germany).

### Assessment and quantification of immunoreactivity

The presence and localisation of  $\alpha\text{Syn}$  pathology were assessed in 99 donors. Per case, a total of four sections were immunostained: three sections of the superior retina immunostained with LB509, pSer129 and KM51, and one section of the inferior retina using LB509 (Supplementary Fig. 1). For 28 donors, optic nerve tissue was available, which was separately assessed for  $\alpha\text{Syn}$  pathology. Immunostained cross-sections were imaged using an Olympus VS200 slide scanner. With the assessment of LB509, pSer129 and KM51 in the superior retina, LB509 appeared most sensitive in detecting  $\alpha\text{Syn}$  pathological structures (Supplementary Fig. 1a). For this reason and to reduce the chance of sampling bias, the inferior retina was stained with LB509 (Supplementary Fig. 1d). Overall, minor variability in the detection of pathological structures in the retina and optic nerve was observed between the different markers. Retinal and optic nerve tissue was assessed based on dichotomised scoring; if Lewy bodies, Lewy neurites or GCIs were observed in at least one of four cross-sections within a case, it was scored as positive (+). When absent in all cross-sections, the case was scored as negative (–) (Supplementary Table 2). In brain tissue,  $\alpha\text{Syn}$  was assessed using KM51 and immunoreactivity was scored with an Olympus BX41 microscope in different brain regions with total surface areas ranging from 2 to 4  $\text{cm}^2$  per section. Staging according to the new proposed Lewy pathology consensus criteria (LPC)<sup>47</sup> was performed by scoring the brain tissue in a dichotomous manner, resulting in “amygdala-predominant” also encompassing cases with “amygdala-only” presence of  $\alpha\text{Syn}$ <sup>48,49</sup>, “brainstem-predominant”, “limbic” and “neocortical” Lewy pathology. Assessment of  $\alpha\text{Syn}$  pathology in the brain and the retina/optic nerve was performed separately and masked for diagnosis. All figures were composed with GraphPad Prism (RRID: SCR\_002798, version 9.3.1) and Adobe Photoshop (Adobe Systems Incorporated, RRID: SCR\_014199, version 23.5).

### Statistical analysis

Demographical differences between diagnostic groups were studied using a one-way ANOVA for continuous data and Chi-square tests for dichotomous data. Univariable binary logistic regression was performed to examine the effect of independent variables on the presence of  $\alpha\text{Syn}$  pathology in the retina and optic nerve. All analyses were corrected for age at death and sex

and were performed using SPSS Statistics (IBM SPSS Statistics, RRID: SCR\_016479) version 28. A *P* value of <0.05 was considered significant.

## DATA AVAILABILITY

All data generated or analysed during this study are included (see also Supplementary Information files).

Received: 23 March 2023; Accepted: 16 August 2023;  
Published online: 28 August 2023

## REFERENCES

- London, A., Benhar, I. & Schwartz, M. The retina as a window to the brain—from eye research to CNS disorders. *Nat. Rev. Neurol.* **9**, 44–53 (2013).
- Guo, L., Choi, S., Bikkannavar, P. & Cordeiro, M. F. Microglia: key players in retinal ageing and neurodegeneration. *Front. Cell Neurosci.* **16**, 804782 (2022).
- Blanks, J. C., Hinton, D. R., Sadun, A. A. & Miller, C. A. Retinal ganglion cell degeneration in Alzheimer's disease. *Brain Res.* **501**, 364–372 (1989).
- den Haan, J. et al. Amyloid-beta and phosphorylated tau in post-mortem Alzheimer's disease retinas. *Acta Neuropathol. Commun.* **6**, 147 (2018).
- Hart de Ruyter, F. J. et al. Phosphorylated tau in the retina correlates with tau pathology in the brain in Alzheimer's disease and primary tauopathies. *Acta Neuropathol.* **145**, 197–218 (2023).
- Schon, C. et al. Long-term in vivo imaging of fibrillar tau in the retina of P301S transgenic mice. *PLoS ONE* **7**, e53547 (2012).
- Beach, T. G. et al. Phosphorylated alpha-synuclein-immunoreactive retinal neuronal elements in Parkinson's disease subjects. *Neurosci. Lett.* **571**, 34–38 (2014).
- Bodis-Wollner, I., Kozlowski, P. B., Glazman, S. & Miri, S. Alpha-synuclein in the inner retina in parkinson disease. *Ann. Neurol.* **75**, 964–966 (2014).
- Ortuno-Lizaran, I. et al. Phosphorylated alpha-synuclein in the retina is a biomarker of Parkinson's disease pathology severity. *Mov. Disord.* **33**, 1315–1324 (2018).
- Ortuno-Lizaran, I. et al. Dopaminergic retinal cell loss and visual dysfunction in Parkinson disease. *Ann. Neurol.* **88**, 893–906 (2020).
- Spillantini, M. G. et al. Alpha-synuclein in Lewy bodies. *Nature* **388**, 839–840 (1997).
- Koga, S., Sekiya, H., Kondru, N., Ross, O. A. & Dickson, D. W. Neuropathology and molecular diagnosis of synucleinopathies. *Mol. Neurodegener.* **16**, 83 (2021).
- Yang, Y. et al. Structures of alpha-synuclein filaments from human brains with Lewy pathology. *Nature* **610**, 791–795 (2022).
- Shy, G. M. & Drager, G. A. A neurological syndrome associated with orthostatic hypotension: a clinical-pathologic study. *Arch. Neurol.* **2**, 511–527 (1960).
- Lashuel, H. A., Overk, C. R., Oueslati, A. & Masliah, E. The many faces of alpha-synuclein: from structure and toxicity to therapeutic target. *Nat. Rev. Neurosci.* **14**, 38–48 (2013).
- Killingler, B. A., Melki, R., Brundin, P. & Kordower, J. H. Endogenous alpha-synuclein monomers, oligomers and resulting pathology: let's talk about the lipids in the room. *NPJ Parkinsons Dis.* **5**, 23 (2019).
- Fujiwara, H. et al. alpha-Synuclein is phosphorylated in synucleinopathy lesions. *Nat. Cell Biol.* **4**, 160–164 (2002).
- Anderson, J. P. et al. Phosphorylation of Ser-129 is the dominant pathological modification of alpha-synuclein in familial and sporadic Lewy body disease. *J. Biol. Chem.* **281**, 29739–29752 (2006).
- Leger, F. et al. Protein aggregation in the aging retina. *J. Neuropathol. Exp. Neurol.* **70**, 63–68 (2011).
- Martinez-Navarrete, G. C., Martin-Nieto, J., Esteve-Rudd, J., Angulo, A. & Cuenca, N. Alpha synuclein gene expression profile in the retina of vertebrates. *Mol. Vis.* **13**, 949–961 (2007).
- Ho, C. Y., Troncoso, J. C., Knox, D., Stark, W. & Eberhart, C. G. Beta-amyloid, phospho-tau and alpha-synuclein deposits similar to those in the brain are not identified in the eyes of Alzheimer's and Parkinson's disease patients. *Brain Pathol.* **24**, 25–32 (2014).
- Sorrentino, Z. A. et al. Unique alpha-synuclein pathology within the amygdala in Lewy body dementia: implications for disease initiation and progression. *Acta Neuropathol. Commun.* **7**, 142 (2019).
- Toft-Kehler, A. K., Skytt, D. M. & Kolko, M. A perspective on the Müller cell-neuron metabolic partnership in the inner retina. *Mol. Neurobiol.* **55**, 5353–5361 (2018).
- Indrieri, A., Pizzarelli, R., Franco, B. & De Leonibus, E. Dopamine, alpha-synuclein, and mitochondrial dysfunctions in parkinsonian eyes. *Front. Neurosci.* **14**, 567129 (2020).
- Mendoza-Santesteban, C. E., Gabilondo, I., Palma, J. A., Norcliffe-Kaufmann, L. & Kaufmann, H. The retina in multiple system atrophy: systematic review and meta-analysis. *Front. Neurol.* **8**, 206 (2017).
- Jellinger, K. A. Is Braak staging valid for all types of Parkinson's disease? *J. Neural Transm.* **126**, 423–431 (2019).
- Braak, H. et al. Staging of brain pathology related to sporadic Parkinson's disease. *Neurobiol. Aging* **24**, 197–211 (2003).
- Robinson, J. L. et al. The development and convergence of co-pathologies in Alzheimer's disease. *Brain* **144**, 953–962 (2021).
- Urwyler, P. et al. Visual hallucinations in eye disease and Lewy body disease. *Am. J. Geriatr. Psychiatry* **24**, 350–358 (2016).
- Esmaeeli, S. et al. Visual hallucinations, thalamocortical physiology and Lewy body disease: a review. *Neurosci. Biobehav. Rev.* **103**, 337–351 (2019).
- Erskine, D. et al. Pathological changes to the subcortical visual system and its relationship to visual hallucinations in dementia with Lewy bodies. *Neurosci. Bull.* **35**, 295–300 (2019).
- Ravid, R. & Swaab, D. F. The Netherlands brain bank—a clinico-pathological link in aging and dementia research. *J. Neural Transm. Suppl.* **39**, 143–153 (1993).
- Klioueva, N. M. et al. BrainNet Europe's Code of Conduct for brain banking. *J. Neural Transm.* **122**, 937–940 (2015).
- Alafuzoff, I. et al. Staging/typing of Lewy body related alpha-synuclein pathology: a study of the BrainNet Europe Consortium. *Acta Neuropathol.* **117**, 635–652 (2009).
- Montine, T. J. et al. National Institute on Aging-Alzheimer's Association guidelines for the neuropathologic assessment of Alzheimer's disease: a practical approach. *Acta Neuropathol.* **123**, 1–11 (2012).
- Thal, D. R., Rub, U., Orantes, M. & Braak, H. Phases of A beta-deposition in the human brain and its relevance for the development of AD. *Neurology* **58**, 1791–1800 (2002).
- Hyman, B. T. et al. National Institute on Aging-Alzheimer's Association guidelines for the neuropathologic assessment of Alzheimer's disease. *Alzheimers Dement.* **8**, 1–13 (2012).
- Braak, H. & Braak, E. Neuropathological staging of Alzheimer-related changes. *Acta Neuropathol.* **82**, 239–259 (1991).
- Mirra, S. S. et al. The Consortium to Establish a Registry for Alzheimer's Disease (CERAD). Part II. Standardization of the neuropathologic assessment of Alzheimer's disease. *Neurology* **41**, 479–486 (1991).
- McKeith, I. G. et al. Diagnosis and management of dementia with Lewy bodies: Fourth Consensus Report of the DLB Consortium. *Neurology* **89**, 88–100 (2017).
- Jellinger, K. A. Multiple system atrophy: an oligodendroglioneuronal synucleinopathy. *J. Alzheimers Dis.* **62**, 1141–1179 (2018).
- Jellinger, K. A. Lewy body-related alpha-synucleinopathy in the aged human brain. *J. Neural Transm.* **111**, 1219–1235 (2004).
- Dickson, D. W. et al. Office of Rare Diseases neuropathologic criteria for corticobasal degeneration. *J. Neuropathol. Exp. Neurol.* **61**, 935–946 (2002).
- Duyckaerts, C. et al. PART is part of Alzheimer disease. *Acta Neuropathol.* **129**, 749–756 (2015).
- Kovacs, G. G. et al. Aging-related tau astroglial pathology (ARTAG): harmonized evaluation strategy. *Acta Neuropathol.* **131**, 87–102 (2016).
- Delic, V. et al. Sensitivity and specificity of phospho-Ser129 alpha-synuclein monoclonal antibodies. *J. Comp. Neurol.* **526**, 1978–1990 (2018).
- Attems, J. et al. Neuropathological consensus criteria for the evaluation of Lewy pathology in post-mortem brains: a multi-centre study. *Acta Neuropathol.* **141**, 159–172 (2021).
- Uchikado, H., Lin, W. L., DeLucia, M. W. & Dickson, D. W. Alzheimer disease with amygdala Lewy bodies: a distinct form of alpha-synucleinopathy. *J. Neuropathol. Exp. Neurol.* **65**, 685–697 (2006).
- Leverenz, J. B. et al. Empiric refinement of the pathologic assessment of Lewy-related pathology in the dementia patient. *Brain Pathol.* **18**, 220–224 (2008).

## ACKNOWLEDGEMENTS

We want to acknowledge all donors and their caregivers. We thank the Netherlands Brain Bank for providing well-characterised brain tissue and eyes. We thank Michiel Kooreman (Netherlands Brain Bank) for helping with clinical data retrieval and collecting brain sections. We thank N.P. Smoor for his technical expertise and assistance in retinal tissue preparation. Alzheimer Nederland, AN-project WE.03-2021-14 partly funded this study. The funder played no role in the study design, data collection, data analysis and interpretation, or this manuscript's writing.

## AUTHOR CONTRIBUTIONS

F.J.H.d.R., T.H.J.M., J.d.H., J.F.d.B., P.S., F.H.B., F.D.V., A.J.M.R. and J.J.M.H. contributed to the conception and design of the study. Experiments were performed by T.H.J.M. and



G.G. F.J.H.d.R. performed data collection and analysis. F.J.H.d.R. and J.W.R.T. performed statistical analysis. J.d.H., J.F.d.B., P.S., F.H.B., F.D.V., A.J.M.R. and J.J.M.H. supported data interpretation. The first draft of the manuscript was written by F.J.H.d.R. and J.J.M.H. All authors commented on previous versions of the manuscript. All authors read and approved the final manuscript.

## COMPETING INTERESTS

J.F.d.B. has acquired grant support (for the institution; Department of Physics, VU) from the Dutch Research Council (NWO) and industry (Thorlabs, ASML, Heidelberg Engineering). He has received royalties related to IP on OCT technologies and semiconductor metrology. He has acted as an expert witness for a UK-based law firm; P.S. has received consultancy fees (paid to the university) from Alzheon, Brainstorm Cell and Green Valley. Within his university affiliation, he is the global PI of the phase 1b study of AC Immune, Phase 2b study with FUJI-film/Toyama and phase 2 study of UCB and phase 1 study with ImmunoBrain Checkpoint. He is chair of the EU steering committee of the phase 2b programme of Vivoryon, the phase 2b study of Novartis Cardiology and co-chair of the phase 3 study with NOVO-Nordisk. He is also an employee of EQT Life Sciences (formerly LSP); F.B. performs contract research for Optina Dx and Optos; she has been an invited speaker at Roche and has been invited for expert testimony at Biogen. All funding is paid to her institution; J.J.M.H. received grants from the Dutch Research Council (ZonMW), and, Alzheimer Netherlands, performed contract research or received grants from Merck, ONO Pharmaceuticals, Janssen Prevention Center, DiscovericBio, AxonNeurosciences, Roche, Genentech, Promis, Denali, FirstBiotherapeutics, and Ensol Biosciences. All payments were made to the institution. J.J.M.H. participates in the scientific advisory board of Alzheimer Netherlands and is Editor-in-Chief for *Acta Neuropathologica Communications*. The other authors declare no competing interests.

## ADDITIONAL INFORMATION

**Supplementary information** The online version contains supplementary material available at <https://doi.org/10.1038/s41531-023-00570-5>.

**Correspondence** and requests for materials should be addressed to Jeroen J. M. Hoozemans.

**Reprints and permission information** is available at <http://www.nature.com/reprints>

**Publisher's note** Springer Nature remains neutral with regard to jurisdictional claims in published maps and institutional affiliations.



**Open Access** This article is licensed under a Creative Commons Attribution 4.0 International License, which permits use, sharing, adaptation, distribution and reproduction in any medium or format, as long as you give appropriate credit to the original author(s) and the source, provide a link to the Creative Commons license, and indicate if changes were made. The images or other third party material in this article are included in the article's Creative Commons license, unless indicated otherwise in a credit line to the material. If material is not included in the article's Creative Commons license and your intended use is not permitted by statutory regulation or exceeds the permitted use, you will need to obtain permission directly from the copyright holder. To view a copy of this license, visit <http://creativecommons.org/licenses/by/4.0/>.

© The Author(s) 2023